Received 15 December 2019; revised 10 February 2020; accepted 25 February 2020. Date of publication 27 February 2020; date of current version 10 March 2020. The review of this paper was arranged by Editor S. Reggiani.

Digital Object Identifier 10.1109/JEDS.2020.2976637

Effective Concentration Profile: A Novel 1-D Analysis of the Variation of Lateral Thickness (VLT) Lateral Power Devices

JUN ZHANG [1,2,3] (Member, IEEE), YU-FENG GUO [1,2] (Member, IEEE), CHEN-YANG HUANG [1,2], AND FANG-REN HU [1,2]

1 College of Electronic Science and Engineering, Nanjing University of Posts and Telecommunications, Nanjing 210003, China
2 National and Local Joint Engineering Laboratory for RF Integration and Micro-Packaging Technologies, Nanjing University of Posts and Telecommunications, Nanjing 210003, China
3 State Key Laboratory of Electronic Thin Films and Integrated Devices, University of Electronic Science and Technology of China, Chengdu 610054, China

CORRESPONDING AUTHOR: Y.-F. GUO (e-mail: yfguo@njupt.edu.cn)

This work was supported in part by the China Post-Doctoral Science Foundation under Grant 2018M642291, in part by the Natural Science Foundation of Jiangsu Province under Grant BK20190237, in part by the Opening Project of State Key Laboratory of Electronic Thin Films and Integrated Devices under Grant KFJJ201907, and in part by the National Natural Science Foundation of China under Grant 6190030245, Grant 61574081, and Grant 61704084.

ABSTRACT The VLT technique features for its irregular thickness of drift region and therefore realize the even surface electric field even with a uniformly doped drift region. However, the sophisticated structure of the drift region also making 2-D methods impractical in both modeling and explaining VLT's physical nature. In this paper, based on the Effective Concentration Profile (ECP) theory, a simple but effective 1-D modeling methodology is proposed to provide physical insight into the VLT technique. The VLT-ECP concept indicates that by physically removing the region that above Charge Appointment Line (CAL), the charge contributes to the lateral depletion can be reduced to zero leading to an even surface electric field. Further, an optimization criterion is proposed to provide useful guidance for the designing of VLT lateral power devices in practice. The comparison between the analytical results obtained by the proposed model and TCAD simulations verified the veracity and effectiveness of the proposed methodology.

INDEX TERMS Variation of lateral thickness, 1-D model, effective concentration profile, breakdown voltage, lateral power device.

I. INTRODUCTION

The development of lateral power device has made revolutionary progress as the introduction of Reduce Surface Electric Field (RESURF) technique, which improves the lateral breakdown voltage (BV) with the help of 2-D coupling effect between lateral and vertical structure [1]–[4]. To further utilize such 2-D coupling effect and obtain a better trade-off between breakdown voltage and specific on-resistance (Ron), many important techniques have been introduced to push the device operates closer to the ideal switch that features infinite electrical conductivity or resistivity when turned on or off. Among them, the most direct approach is to alter the charge distribution ($Q(x) = N_d(x) \times t_s(x)$) of drift region [4]–[8]. This concept further stimulates the revolutionary techniques such as Variable of Lateral Diffusion (VLD) and Variable of Lateral Thickness (VLT). Both the VLD and VLT are featured as their ability to achieve an even surface electric field profile and the most desirable lateral BV characteristic [10]–[12]. Due to the linear doping profile of VLD, a lightly doped drift region near the PN junction is formed which inevitably causes severe local self-heating and on-state characteristic deterioration [7], [9]. Moreover, the fabrication of VLD devices requires perforated mask layout and long-time/high- temperature annealing which increases costs and reduces yields [7], [9]. To avoid those drawbacks of VLD, VLT technique has been introduced which alter the drift region lateral charge distribution via variation of its thickness rather than doping. Yet, the 2-D structure of VLT device also brings enormous difficulties in 2-D modeling

This work is licensed under a Creative Commons Attribution 4.0 License. For more information, see http://creativecommons.org/licenses/by/4.0/

and analysis owing to the irregular shape of the drift region [6], [7]. For the 2-D solutions, the 2-D Poisson's equation is now a semi-homogenous equation as a result of variable drift region thickness. The direct solving of this semi-homogeneous equation further leads to the usage of modified Bessel function making a very much difficult modeling process [6], [13]. Such a sophisticated 2-D model is impractical both in explaining the physical nature and in exploring the sensitivity of BV characteristic on device parameters.

In this paper, a simple and clear VLT-ECP concept is proposed to explore the VLT technique with veracity and simplicity. The VLT-ECP concept indicates that the inherent 2-D device with varied drift region thickness can be equivalent to a 1-D planer junction with graded doping in accordance with the ECP. So that the complicated modeling processes of 2-D approaches are been bypassed making the modeling difficulties of VLT devices reduced significantly. Using the proposed 1-D VLT-ECP concept, a 1-D analytical model is proposed to depict the surface electric field profile and BV of the VLT lateral power devices. Based on the proposed model, a simple optimization method is proposed to provide design guidance so that the most desirable BV characteristic can be achieved. The results obtained by the proposed model are found to be sufficiently accurate comparing with simulation results by MEDICI, technology computer-aided design (TCAD) tool. The simulation models used in MEDICI are CONSRH, AUGER, BGN, FLDMOB, IMPACT.I and CCSMOB.

II. EFFECTIVE CONCENTRATION PROFILE

The lateral power device sustains applied reverse-voltage mainly via the depletion of the drift region. Therefore, the doping dose of the drift region takes a dominant role in affecting the device off-state characteristics. The VLT technique optimizes the doping dose of drift region via the change of drift region thickness. In this paper, the 2-D cross-section of the lateral power device using VLT technique for modeling is shown in Fig. 1 (a). When the device operates in the off-state, both the VLT effect and 2-D RESURF effect lay their influence on the depletion of the drift region. By using the second-order Taylor series expansion along the y dimension to approximate the electric potential in the depletion region, a general differential equation for the surface electric potential $[\varphi(x,0)]$ can be expressed as:

$$\frac{\partial^2\varphi(x,0)}{\partial x^2}+\frac{\varphi(x,0)}{Kt_{ox}t_d(x)}=-\frac{qN_d}{\varepsilon_s} \tag{1}$$

where the t_{ox} and $t_d(x)$ are the thickness of buried oxide (BOX) layer and drift region, q is the electronic charge, N_d being the drift region doping concentration, ε_s and ε_{ox} is the dielectric constant of Silicon and Silicon Dioxide material, respectively. $K=\varepsilon_s/\varepsilon_{ox}\sim 3$ represents the dielectric constant ratio of silicon and silicon dioxide material. To solve Eq. (1) directly, the modified Bessel function and the composite Bessel function have to be introduced making the

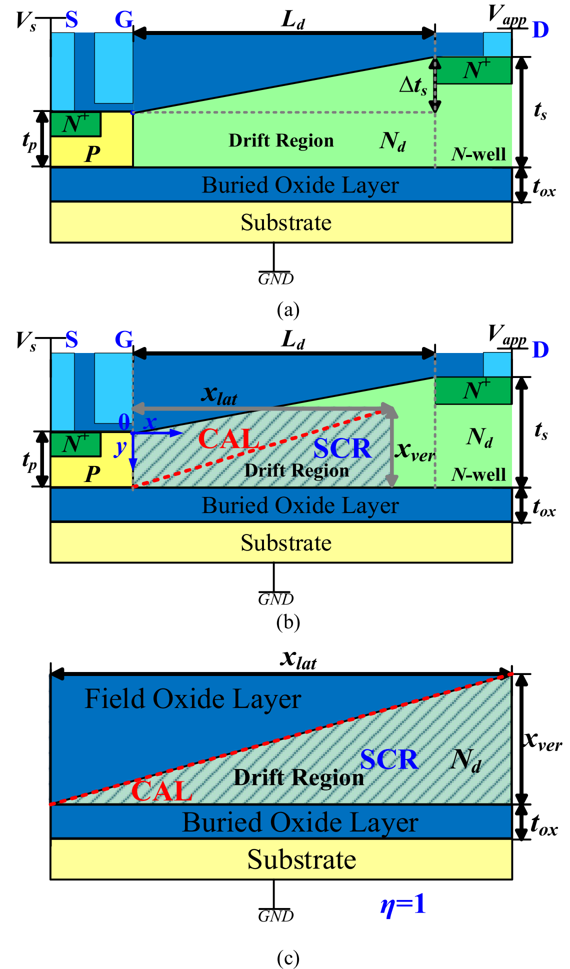

FIGURE 1. **(a). 2-D cross-section of the SOI LDMOS with VLT structure, (b). the ECP equivalent structure for modeling (*x-y* plane) and (c). the ideal VLT case (no charges in the drift region for lateral depletion).**

correspondent mathematical expressions for surface electric field and potential can only be given by the non-elementary functions [6], [13]. On the other hand, by employing the ECP concept, the influence of VLT and 2-D RESURF effect can be equivalent to the increment on effective concentration in the drift region, respectively. Thus, the effective concentration profile ($N_{eff}(x)$) can be easily obtained by using the principle of compensation semiconductor, which yields:

$$N_{eff}(x)=N_d+\Delta N_{eff-RESURF}+\Delta N_{eff-VLT} \tag{2}$$

where $\Delta N_{eff-RESURF}=-\eta xN_d/Min[x_{lat},L_d]$ indicates the influence of the 2-D coupling effect on ECP [4]. In this paper, $\eta=x_{ver}(V_{app})/t_s$ is the ratio of vertical depletion length at $x=Min[x_{lat},L_d]$ and SOI layer thickness. Barring the 2-D RESURF effect caused by BOX and substrate layers, the influence of thickness function on doping dose satisfies $Q(x)=N_d\times t_d(x)$. For the purpose of dimensional reduction, the doping dose function can be further re-written as $Q(x)=N(x)\times t_s$. Obviously, the effective doping concentration increment induced by drift region thickness ought to satisfies $N(x)=N_d+\Delta N_{eff-VLT}=N_d\times t_d(x)/t_s$. The actual

VLT structure shown in Fig. 1 (a) can be equivalent to a lateral power device with varied drift region doping, and the overall ECP can be therefore given as:

$$N_{eff}(x) = N(x) - N_d \cdot \eta \frac{x}{Min[x_{lat}, L_d]} \tag{3}$$

As the Eq. (3) indicates, the coupling between the 2-D RESURF effect and varied thickness determines the ECP. In off-state case, the reverse-biased voltage is applied which causes the lateral and vertical depletions to occur simultaneously. As shown in Fig. 1 (b), the inevitable overlap of depletion between the lateral and vertical structures formed a Sharing Charge Region (SCR). The length and height of SCR are therefore defined by the width of the lateral and vertical depletion region, namely x_{lat} and x_{ver}, respectively. A Charge Appointment Line (CAL) divides the charges in SCR into two parts, only the upper part contributes to the lateral depletion. According to REF [4] and [12], the CAL satisfies $\text{CAL}(x) = \eta x N_d / Min[x_{lat}, L_d]$. As Fig. 1 (b) intuitively shows, by using the Eq. (3), the VLT structure can be understood as by physically removing the charge in SCR, the equivalent doping concentration for the lateral breakdown is reduced and therefore an evener surface electric field can be realized.

Theoretically, for an ideal VLT case, the drift region thickness is a linear function [6], [7]. As Eq. (3) indicates, if the drift region edge coincident with the CAL, namely the drift region thickness function $t_d(x)$ satisfies $t_{d_opt}(x) = (x/L_d)t_s$, the $N_{eff}(x) = 0$. In this case, the drift region just fully depleted, namely $\eta = 1$. As shown in Fig. 1 (c), which means all the charges in the drift region are allocated to the vertical junction when the drift region is fully depleted. Since there is no charge contributes to the lateral depletion, for the lateral structure, the drift region can be equivalently treated to be intrinsic and therefore an even surface electric field and ideal BV characteristic can be obtained.

However, the biggest challenge is the fabrication especially the realization of drift region thickness that defined by a proportional function. Since in practice, the thickness of P-well is impossible to be zero ($t_p \neq 0$). In this case, the actual drift region thickness is, therefore, can be given as:

$$t_d(x) = \frac{x}{L_d} \Delta t_s + t_p \tag{4}$$

In fact, as indicated in Eq. (3), both the drift region thickness and the 2-D RESURF effect play a decisive role in affecting the BV characteristic of VLT lateral power devices. To make the most of the VLT technique, the designing optimization criterion for practical VLT devices ought to be provided so that the optimized off-state performance can be achieved.

So far, by utilizing the ECP concept in VLT lateral power devices, the inherent 2-D problem has now reduced to a simple 1-D problem which can be described by directly solving 1-D Poisson's equation yielding:

$$\frac{d^2\varphi(x, 0)}{dx^2} = \frac{dE(x, 0)}{dx} = -\frac{qN_{eff}(x)}{\varepsilon_s} \tag{5}$$

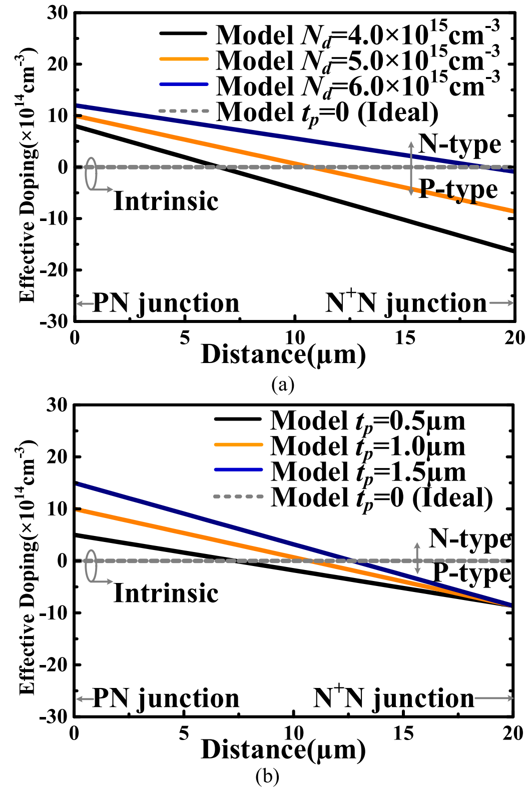

FIGURE 2. Effective Doping Concentration of the drift region for various (a). drift region doping concentration (V_{app} = 400V, t_p = 1.0μm), (b). thickness of P-well (V_{app} = 400V, N_d = 5.0 × 10^{15}cm^{-3}) with t_s = 7μm, t_{ox} = 3μm, L_d = 20μm.

Fig. 2 intuitively shows the influence of 2-D coupling between the VLT and RESURF effects on ECP. Since the actual drift region thickness near the PN junction excess the $t_{d_opt}(x)$, the extra charges will contribute to the lateral depletion. Accordingly, the ECP in the drift region can no longer be intrinsic and thus sabotaging the ideal surface electric field profile. As shown in Fig. 2 (a), such a non-ideal ECP gets worse with the increase of drift region doping concentration. Obviously, the non-zero P-well thickness is been attributed to the mismatch between the CAL and equivalent doping dose in the drift region. As indicated in Fig. 2 (b), although the thicker P-well intensify such mismatch, the symmetrical under- and over-estimation of drift region charges help to increase the actual doping concentration and realize the optimized surface electric field whose electric field peaks both have the same height. Moreover, as shown in Fig. 2, due to the different types of mismatch between CAL(x) and $t_d(x)$, the equivalent structure of the drift region under full-depletion condition can be divided into two cases. As Fig. 3 (a) shows, if the field oxide(FOX) layer boundary above CAL ($\eta = 1$), the excessive charges in drift region form an equivalent N-type region, and thus creating an electric field peak at the PN junction. Whereas for the case that $\eta >\ 1$, the cross between CAL(x) and $t_d(x)$ leads to an equivalent N(x)P(x) drift region which stimulates

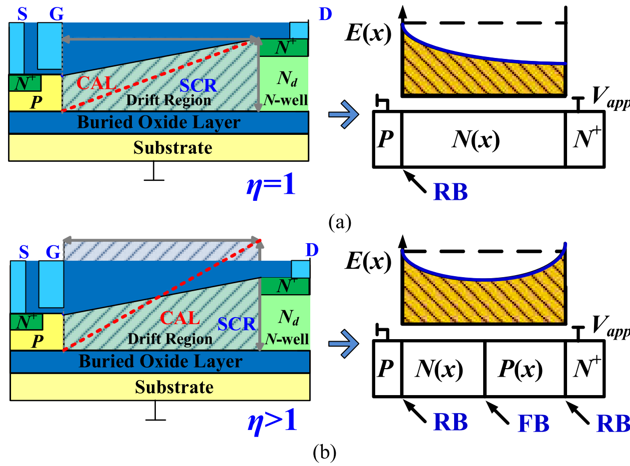

FIGURE 3. Effective lateral structure and the electric field distribution of the VLT device at: (a). N-type and (b). NP-type drift region (RB: Reverse-Biased, FB: Forward-Biased).

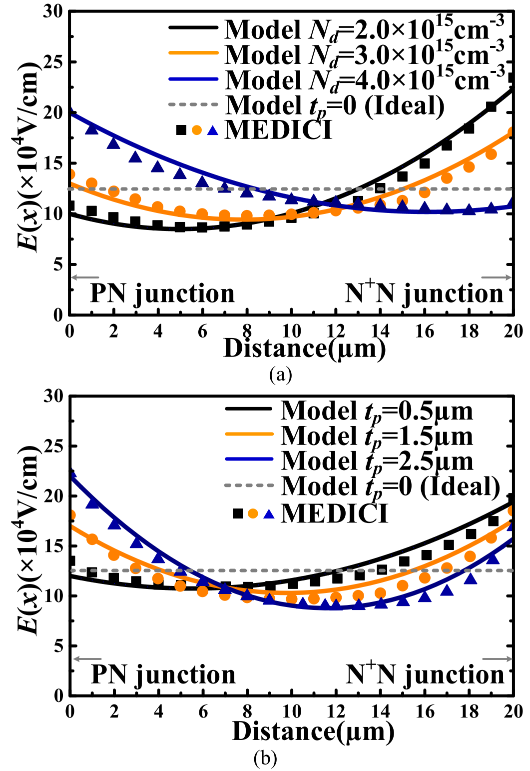

FIGURE 4. Analytical and numerical surface electric field profiles of the drift region under a unified coordinate axis for various (a). Drift region doping (V_{app} = 250V, t_p = 1μm), (b). P-well thickness (V_{app} = 250V, N_d = 3.0 × 10^{15}cm^{-3}) with t_s = 5μm, t_{ox} = 2μm, L_d = 20μm.

a new electric field peak occurs at NN$^+$ junction. Especially, when a strong 2-D RESURF effect exists and $\eta > 2$, the absolute value of ECP reaches its maximum at $x = L_d$. Therefore, same as that in Single/Double RESURF devices, the surface electric field peak at NN$^+$ junction is expected to excesses the one at PN junction [4], [14]. As a result of the thickness of P-well, the intrinsic ECP of the drift region is impossible to be achieved. So that, the perfectly even surface electric field shall no occur.

III. SURFACE ELECTRIC FIELD

A. SURFACE ELECTRIC FIELD PROFILE

By using the ECP concept, the inherent 2-D VLT structure is equivalent to a 1-D graded junction whose doping is defined by ECP that determined by Eq. (3). Since the lateral breakdown happens on the surface, the analysis of surface electric field profile is essential for the purpose of achieving the desirable device's BV. In a commercial lateral power device, in order to meet the requirement of maintaining a high BV and area utilization rate, the drift region ought to fulfill the full depletion condition. Accordingly, the surface electric field profile of which can be easily obtained by submitting Eq. (3) into Eq. (5), which yields:

$$E(x) = E_0 - \frac{qN_d}{\varepsilon_s}\left[\int \frac{t_d(x)}{t_s}dx - \eta\frac{x^2}{2L_d}\right] \tag{6}$$

where $E_0 = E(0)$ represent the surface electric field at PN junction. As Eq. (7) indicates, the even surface electric field profile can only be obtained when $t_d(x)$ is a proportional function. If the $t_d(x)$ satisfies Eq. (4), the surface electric field profile can be further given as:

$$E(x) = E_0 - \frac{qN_d}{\varepsilon_s}\left[\frac{x^2}{2L_d}\left(\frac{\Delta t_s}{t_s} - \eta\right) + \left(1 - \frac{\Delta t_s}{t_s}\right)\cdot x\right] \tag{7}$$

As shown in Fig. 4, the non-ideal structure of the drift region significantly sabotages the surface electric field. Since the distance along the FOX boundary is slightly longer than the drift region length, for the purpose of simplicity, the simulated surface electric field that obtained along the FOX boundary and analytical results are presented with a unified coordinate axis. The Fig. 4 (a) indicates that the excessive charges near the PN and NN$^+$ junctions promote electric field crowding at PN and NN$^+$ junction, respectively. Apparently, a higher N_d curbs the appearance of the equivalent P-type region, therefore, reduces the electric field peak at NN$^+$ junction while increases the one at PN junction. The P-well thickness, on the other hand, changes the bending degree of surface electric field profile. As shown in Fig. 4 (b), a thicker P-well indicates a small difference between t_s and t_p. Moreover, when $t_s = t_p$, the VLT device is reduced to a conventional Single RESURF device in which case the difference between surface electric field peak and valley reaches its maximum.

B. SURFACE ELECTRIC FIELD OPTIMIZATION

As discussed above, in order to maximize the optimized lateral BV characteristic, the electric field crowding at both PN and NN$^+$ junctions ought to be adjusted so that any one of which would not reaches the critical electric field (E_C) first. Since the two electric field peak of PN and NN$^+$ junctions is inevitable, the best scenario is to make these two peaks on the surface of drift region reach E_C simultaneously, namely:

$$E(0) = E(L_d) = E_C \tag{8}$$

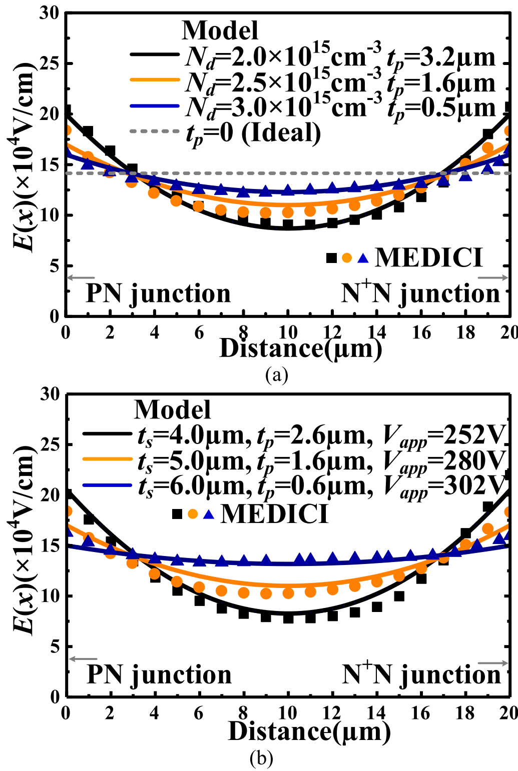

FIGURE 5. **Analytical and numerical surface electric field profiles using the geometric optimization criterion under a unified coordinate for various (a). Drift region doping (V_{app}=280V, t_s = 5μm), (b). Epitaxial layer thickness (N_d = 2.5 × 10^{15}cm^{-3}) with t_{ox} = 2μm, L_d = 20μm.**

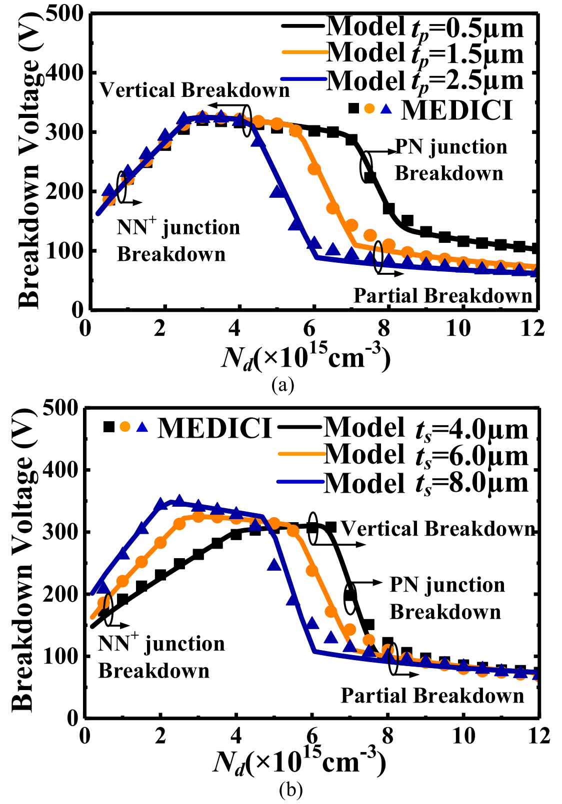

FIGURE 6. **The dependence of breakdown voltage on drift region doping with various (a). P-well thickness(t_s = 6.0μm) and (b). Epitaxial layer thickness (t_p = 1.5μm) with t_{ox} = 2μm, L_d = 20μm.**

Hence, the geometric optimization criterion to achieve the optimized surface electric field can be obtained by submitting Eq. (8) into (7), which yields:

$$t_p/t_s = \eta - 1 \tag{9}$$

As Eq. (9) indicates, in order to achieve the surface electric field symmetrical along the midline of the drift region, the vertical structure of the drift region is determined by the 2-D coupling factor η. For the ideal VLT structure, as shown in Fig. 1 (c), the perfectly even electric field is achieved when the drift region just fully depleted ($\eta = 1$). Obviously, in this case, the surface electric field at both $x = 0$ and L_d has the same height, and therefore as Eq. (9) indicates t_p ought to be zero. Whereas when $t_p = t_s$, the device is now becoming a classic Single RESURF lateral power device whose optimized η can be also obtained via Eq. (9) with $\eta = 2$. Apparently, these conclusions are in accordance with the conventional theories [6]–[7], [14] In fact, the V_{app} vertical structure sustains can be given as:

$$V_{app} = \frac{qN_d t_s}{\varepsilon_s}\left(K\eta t_{ox} + \frac{2\eta - 1}{2}t_s\right) \tag{10}$$

Since the vertical and lateral sustain the same V_{app} simultaneously, the geometric optimization criterion can be further given by submitting Eq. (10) into (9):

$$t_p/t_s = \left(\frac{V_{app} - V_0}{V_0}\right)\cdot\left(\frac{2t^2}{2t^2 + t_s^2}\right) \tag{11}$$

where $t = (0.5{t_s}^2 + Kt_{ox}t_s)^{0.5}$ being the characteristic thickness and $V_0 = qN_d t^2/\varepsilon_s$. Furthermore, by using vertical breakdown condition the optimization criterion can be further simplified as:

$$t_p = \frac{\varepsilon_s E_C}{qN_d} - t_s \tag{12}$$

So far, with the help of geometric optimization criterion, the surface electric field crowding induced by depletion mismatch can be suppressed significantly. Hence, the breakdown voltage of the VLT lateral power device can achieve its maximum. Fig. 5 intuitively shows the optimized surface electric field profile after applying the geometric optimization criterion. The consistency between the analytical results and the simulations validates the veracity and effectiveness of the proposed 1-D methodology. As shown in Fig. 5, with the usage of optimization criterion, the surface electric field is being symmetrical along the midline of the drift region. Only the bending degree of the surface electric field affects the lateral BV characteristic. Fig. 5 (a) also indicates that a thinner P-well may allow a higher drift region doping concentration. Moreover, as shown in Fig. 5 (b), the thickener

the epitaxial layer is the thinner the optimized P-well thickness is. According to the proposed model, it can be reckoned as a larger t_s means the vertical depletion is harder to proceed. Therefore, only a smaller η can be obtained resulting in the CAL in the drift region is more tends to the case of ideal VLT, and an evener surface electric field can be achieved. Although a better lateral BV and Ron trade-off may be achieved by increasing the epitaxial layer thickness, it also brings a bad thermal performance and, if the structure parameters are poorly designed, may even curb the vertical breakdown from happening. More importantly, it is actually desirable to make the device happens vertical breakdown in order to maintain a high BV while achieving a big process tolerance.

IV. BREAKDOWN VOLTAGE

The capability of sustaining reverse biased applied voltage reflects core performance for a lateral power device. The weakest one in BV between the lateral and vertical structure limits the off-state characteristic of the device. As discussed above, electric peaks of the VLT lateral power device occur at (a). Si-SiO$_2$ interface under the drain region; (b). PN junctions and (c). NN$^+$ junction. For a fully depleted drift region, the same as the Single RESURF case, the lateral BV of PN and NN$^+$ junction breakdown can be therefore obtained by submitting Eq. (7) into 1-D Poisson's equation, which yields:

$$\text{PN junction: } BV_{lat}^{FPN} = E_C L_d - \frac{qN_d L_d^2}{2\varepsilon_s}\left(1 - \frac{\eta}{3} - \frac{2}{3}\frac{\Delta t_s}{t_s}\right) \quad (13)$$

$$\text{NN}^+\text{ junction: } BV_{lat}^{FNN} = E_C L_d - \frac{qN_d L_d^2}{2\varepsilon_s}\left(\frac{2\eta}{3} - 1 + \frac{1}{3}\frac{\Delta t_s}{t_s}\right) \quad (14)$$

In this paper, the critical electric field (E_C) is determined by $E_C = 3.0 \times 10^5/[1 - 0.33\ \log_{10}\ (N_d/10^{16})]$ (V/cm) [4], [5], [12], [13]. It is worth to be noted that the proposed method can also be applied to the partial depletion case. To do so, L_d used in Eq. (7) and (13) should be replaced by x_{lat} which is given by $\int E(x)dx = V_{app}$ and $E(x_{lat}) = 0$. However, as shown in Fig. 6, partial depletion breakdown ought to be avoided during the designing phase for its rather low breakdown voltage [12]. Therefore, we will not discuss partial depletion case in detail within the scope of this paper. As for the vertical structure, in light of the full depletion requirement, the vertical breakdown voltage can be given as:

$$BV_{ver} = E_C(Kt_{ox} + t_s) - \frac{qN_d t_s^2}{2\varepsilon_s} \quad (15)$$

So far, the lateral and vertical breakdown voltages are obtained using the proposed 1-D VLT-ECP model. Thus, the overall breakdown voltage can be given by using the lowest among BV_{lat} and BV_{ver}, which yields:

$$BV = Min[BV_{lat}, BV_{ver}] \quad (16)$$

As shown in Fig. 6, same as that of Single/Double RESURF devices, the breakdown of VLT lateral power devices may successively undergo NN$^+$ junction full-depletion breakdown, vertical breakdown, PN junction full depletion breakdown, and PN junction partial-depletion breakdown with the increase of N_d. Nevertheless, as Fig. 6 (a) indicates, due to the linear thickness of the drift region and its modulation effect on charge distribution of drift region, the vertical breakdown is easier to occur allowing a wider range of N_d variation. As the gap between the thickness of epitaxial and P-well widens, the equivalent charge distribution is closer to the ideal VLT case, thus an evener surface electric field may be obtained. As shown in Fig. 6 (a) and (b), such an objective can be achieved by either decreasing the t_p or increasing the t_s. However, as shown in Fig. 6 (b), the thickening of the epitaxial layer also affects the 2-D RESURF effect thus changing the BV-N_d curve in a more sophisticated way. As Fig. 6 (b) shows, the coupling between 2-D RESURF and VLT effects leads to a higher degree of optimization complexity.

In order to provide a theoretical window for optimizing the drift region doping dose($Q = N_d \times t_s$) of a VLT lateral power device, in this paper, we propose an optimized doping dose(ODD) criterion whose limits are determined by vertical and lateral BVs. As shown in Fig. 5, the upper limit (Q_{up}) and the lower limit(Q_{down}) of ODD are determined by the $BV_{ver} - BV_{lat}{}^{FPN}$ and $BV_{ver} - BV_{lat}{}^{FNN}$, respectively. Thus, the optimized doping window of the drift region can be obtained by submitting Eq. (13) and (14) into (15), which yields:

$$Q_{up} = \frac{\varepsilon_s E_C}{q}\left[\frac{6\alpha^2 - 18\alpha\beta + 6\alpha - 1}{3(\alpha^2 - 1 - 2/3 \cdot r)}\right] \quad (17)$$

$$Q_{down} = \frac{\varepsilon_s E_C}{q}\left[\frac{6\alpha^2 - 18\alpha\beta + 6\alpha + 2}{3(\alpha^2 + 1 + 1/3 \cdot r)}\right] \quad (18)$$

where $\alpha = t_s/L_d$, $\beta = t_{ox}/L_d$ and $r = \Delta t_s/L_d$. Similar to the single RESURF case, α and β are the shape factors of the SOI layer and buried oxide layer, respectively. Hereby, the structure optimization criterion can be given as:

$$Q_{down} \le Q \le Q_{up} \quad (19)$$

As Eq. (17) and (18) indicate, compared to the Single/Double RESURF cases, the VLT technique significantly improves upper limit and the drift region process tolerance($\Delta Q = Q_{up} - Q_{down}$). The ΔQ reaches its maximum when the ideal VLT structure is achieved ($r = \alpha$). In which case, the Eq. (17) and (18) become:

$$Q_{up_MAX} = \frac{\varepsilon_s E_C}{q}\left[\frac{6\alpha^2 - 18\alpha\beta + 6\alpha - 1}{3(\alpha^2 - 1 - 2/3 \cdot \alpha)}\right] \quad (20)$$

$$Q_{down_MAX} = \frac{\varepsilon_s E_C}{q}\left[\frac{6\alpha^2 - 18\alpha\beta + 6\alpha + 2}{3(\alpha^2 + 1 + 1/3 \cdot \alpha)}\right] \quad (21)$$

Also, when r equals to zero, the VLT lateral power device degenerates to a Single RESURF device, thus $Q_{up} = Q_{S-up}$ and $Q_{down} = Q_{S-down}$ [4].

V. CONCLUSION

In order to explore the physical meaning of the VLT technique and provide effective design guidance for the practice VLT lateral power device, we proposed a simple but accurate 1-D methodology to depict the sophisticated 2-D problem via ECP theory. The proposed VLT-ECP concept indicates that the VLT technique can be reckoned that achieving the perfectly even surface electric field by equivalently removing the charges above CAL. By doing so, there is no charge in drift region that contribute to lateral depletion, so that to the lateral structure the drift region can be treated as intrinsic. However, since the thickness of P-well cannot be ignored, the ideal VLT structure is impossible to be realized. Therefore, using the proposed VLT-ECP concept, a novel analytical model is presented to qualitatively and quantitatively explore the sensitivity of the surface electric field and breakdown voltage to structure parameters for the first time. Furthermore, a simple but effective geometric optimization criterion is obtained using the proposed 1-D model to provide design guidance. The results obtained by the proposed model both are found to be sufficiently accurate as compared to TCAD simulation results.

REFERENCES

[1] D. Disney, T. Letavic, T. Trajkovic, T. Terashima, and A. Nakagawa, "High-voltage integrated circuits: History, state of the art, and future prospects," *IEEE Trans. Electron Devices*, vol. 64, no. 3, pp. 659–673, Mar. 2017, doi: 10.1109/TED.2016.2631125.

[2] X. R. Luo *et al.*, "Ultralow ON-resistance high-voltage p-channel LDMOS with an accumulation-effect extended gate," *IEEE Trans. Electron Devices*, vol. 63, no. 6, pp. 2614–2619, Jun. 2016, doi: 10.1109/TED.2016.2555327.

[3] F. Udrea, G. Deboy, and T. Fujihira, "Superjunction power devices, history, development, and future prospects," *IEEE Trans. Electron Devices*, vol. 64, no. 3, pp. 713–727, Mar. 2017, doi: 10.1109/TED.2017.2658344.

[4] J. Zhang *et al.*, "One-dimensional breakdown voltage model of SOI RESURF lateral power device based on lateral linearly graded approximation," *Chin. Phys. B*, vol. 24, no. 2, 2015, Art. no. 028502, doi: 10.1088/1674-1056/24/2/028502.

[5] M. Imam, M. Quddus, J. Adams, and Z. Hossain, "Efficacy of charge sharing in reshaping the surface electric field in high-voltage lateral RESURF devices," *IEEE Trans. Electron Devices*, vol. 51, no. 1, pp. 141–148, Jan. 2004, doi: 10.1109/TED.2003.82138.

[6] J. Yao *et al.*, "Analytical model for silicon-on-insulator lateral high-voltage devices using variation of lateral thickness technique," *Jpn. J. Appl. Phys.*, vol. 54, no. 2, 2015, Art. no. 024301, doi: 10.7567/JJAP.54.024301.

[7] Y. Guo, Z. Wang, and G. Sheu, "Variation of lateral thickness techniques in SOI lateral high voltage transistors," in *Proc. Int. Conf. Commun. Circuits Syst.*, Milpitas, CA, USA, 2009, pp. 611–613, doi: 10.1109/ICCCAS.2009.5250456.

[8] S. Liu, R. Ye, W. Sun, and L. Shi, "A novel lateral DMOS transistor with H-shape shallow-trench-isolation structure," *IEEE Trans. Electron Devices*, vol. 65, no. 11, pp. 5218–5221, Nov. 2018, doi: 10.1109/TED.2018.2871501.

[9] Y. Guo, J. Yao, B. Zhang, H. Lin, and C. Zhang, "Variation of lateral width technique in SoI high-voltage lateral double-diffused metal–oxide–semiconductor transistors using high-k dielectric," *IEEE Electron Device Lett.*, vol. 36, no. 3, pp. 262–264, Mar. 2015, doi: 10.1109/LED.2015.2393913.

[10] A. Ferrara, B. K. Boksteen, R. J. E. Hueting, A. Heringa, J. Schmitz, and P. G. Steeneken, "Ideal RESURF geometries," *IEEE Trans. Electron Devices*, vol. 62, no. 10, pp. 3341–3347, Oct. 2015, doi: 10.1109/TED.2015.2460112.

[11] X. Luo *et al.*, "Ultralow ON-resistance SOI LDMOS with three separated gates and high-*k* dielectric," *IEEE Trans. Electron Devices*, vol. 63, no. 9, pp. 3804–3807, Sep. 2016, doi: 10.1109/TED.2016.2589322.

[12] J. Zhang, Y.-F. Guo, D. Z. Pan, and F.-R. Hu, "A new physical understanding of lateral step doping technique via effective concentration profile concept," *IEEE Trans. Electron Devices*, vol. 66, no. 5, pp. 2353–2358, May 2019, doi: 10.1109/TED.2019.2903346.

[13] B. J. Baliga and S. K. Ghandhi, "Analytical solutions for the breakdown voltage of abrupt cylindrical and spherical junctions," *Solid-State Electron.*, vol. 19, no. 9, pp. 739–744, 1976, doi: 10.1016/0038-1101(76)90152-0.

[14] J. Zhang, Y.-F. Guo, D. Z. Pan, K.-E. Yang, X.-J. Lian, and J.-F. Yao, "Effective doping concentration theory: A new physical insight for the double-RESURF lateral power devices on SOI substrate," *IEEE Trans. Electron Devices*, vol. 65, no. 2, pp. 648–654, Feb. 2018, doi: 10.1109/TED.2017.2786139.